Journal of Sound and Vibration (2000) **238**(1), 179–187
doi:10.1006/jsvi.2000.3019, available online at http://www.idealibrary.com on IDEAL®

THE INFLUENCE OF ROTARY INERTIA OF CONCENTRATED MASSES ON THE NATURAL VIBRATIONS OF FLUID-CONVEYING PIPES

M. G. KANG

Department of Mechanical Engineering Education, Andong National University, 388 *Songchun-dong Andong-city, Kyungbuk* 760-749, *Korea*

(*Received* 3 *February* 1999, *and in final form* 23 *March* 2000)

1. INTRODUCTION

The flow-induced vibration in industry fields has been studied for a long time since it always involves a possibility of severe accidents by the several types of vibrations related to a fluid–structure interaction. Although the vibration analysis of a pipe which having some concentrated masses without a fluid flow had been studied early [1–4], the vibration analysis of that case when a fluid flows through a pipe was not until 1970. Hill and Swanson [5] investigated the effect of concentrated masses on the instability of the fluid-conveying cantilever pipe. Chen and Jendrzejczyk [6] experimentally studied the natural frequencies, mode shapes, and critical velocities for the fluid-conveying cantilever pipe with a concentrated mass at the end of the pipe. Wu and Raju [7] proposed that a concentrated mass installed at the mid-span of the simply supported pipe could change natural frequencies and mode shapes. Although some interesting papers [4, 8, 9] regarding the rotary inertia effect of concentrated masses were published, no one introduced it into the flow-induced vibration field.

Therefore, the present study is aimed at the determination of the effect of rotary inertia of concentrated masses on the natural vibrations and instability of a pipe conveying incompressible fluid. For the analysis, three conservative boundary conditions (i.e., supported–supported, clamped–supported, and clamped–clamped) were assumed as shown in Figure 1.

2. THEORY AND NUMERICAL ANALYSIS

The well-known governing equation [10] for the Euler–Bernoulli-type pipe conveying incompressible fluid through x co-ordinate and vibrating y direction becomes

$$EI\frac{\partial^4 y}{\partial x^4} + 2m_f U\frac{\partial^2 y}{\partial t\,\partial x} + m_f U^2\frac{\partial^2 y}{\partial x^2} + (m_f + m_t)\frac{\partial^2 y}{\partial t^2} = 0, \tag{1}$$

where E and I are the modulus of elasticity and the area moment of inertia of the pipe, m_f and m_t are fluid and pipe masses per unit length, and U and t are the constant uniform fluid velocity and time respectively.

0022-460X/00/460179 + 09 $35.00/0

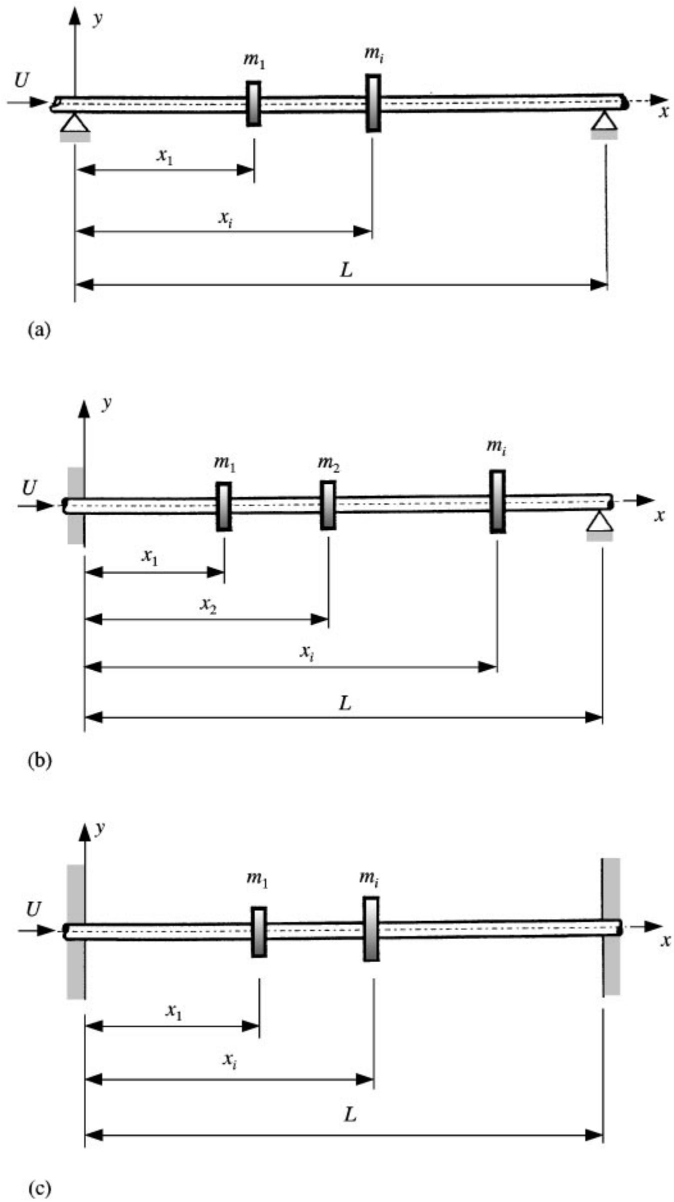

Figure 1. Schematic diagram of the fluid-conveying pipes: (a) supported–supported; (b) clamped–supported; (c) clamped–clamped.

According to Pan [8] and Sato *et al.* [4], the effect of concentrated masses placed at $x = x_i$ can be modelled as follows:

$$\sum_{i=1}^{M} m_i \delta(x - x_i) \frac{\partial^2 y}{\partial t^2} - \frac{\partial}{\partial x}\left\{ \sum_{i=1}^{M} J_i \delta(x - x_i) \frac{\partial^3 y}{\partial x \, \partial t^2} \right\}, \tag{2}$$

where m_i and J_i are the concentrated mass and its rotary inertia and M and δ are the number of concentrated masses and the Dirac delta function respectively. The first equation containing m_i represents the inertia force due to the lateral acceleration of concentrated masses while the second equation containing J_i represents the rotary inertia force due to the angular acceleration of concentrated masses.

Finally, the governing equation for the pipe conveying incompressible fluid and having several concentrated masses can be expressed as

$$EI\frac{\partial^4 y}{\partial x^4} + 2m_f U\frac{\partial^2 y}{\partial t\,\partial x} + m_f U^2\frac{\partial^2 y}{\partial x^2} + \left\{m_f + m_t + \sum_{i=1}^{M} m_i\delta(x - x_i)\right\}\frac{\partial^2 y}{\partial t^2}$$

$$-\frac{\partial}{\partial x}\left\{\sum_{i=1}^{M} J_i\delta(x - x_i)\frac{\partial^3 y}{\partial x\,\partial t^2}\right\} = 0. \tag{3}$$

Introducing dimensionless parameters, equation (3) becomes

$$\frac{\partial^4\eta}{\partial\xi^4} + 2u\beta^{1/2}\frac{\partial^2\eta}{\partial\xi\,\partial\tau} + u^2\frac{\partial^2\eta}{\partial\xi^2} + \left\{1 + \sum_{i=1}^{M}\alpha_i\delta(\xi - \xi_i)\right\}\frac{\partial^2\eta}{\partial\tau^2}$$

$$-\frac{\partial}{\partial\xi}\left\{\sum_{i=1}^{M}\mu_i\delta(\xi - \xi_i)\frac{\partial^3\eta}{\partial\xi\,\partial\tau^2}\right\} = 0, \tag{4}$$

where the dimensionless parameters are

$$\alpha_i = \frac{m_i}{L(m_f + m_t)}, \qquad \beta = \frac{m_f}{m_f + m_t}, \qquad \eta = \frac{y}{L},$$

$$\mu_i = \frac{J_i}{(m_f + m_t)L^3}, \qquad \tau = \left[\frac{EI}{m_f + m_t}\right]^{1/2}\frac{t}{L^2}, \qquad u = \left[\frac{m_f}{EI}\right]^{1/2} UL,$$

$$\xi = \frac{x}{L}, \qquad \xi_i = \frac{x_i}{L}, \qquad \omega = \left[\frac{m_f + m_t}{EI}\right]^{1/2} L^2\Omega.$$

Here, L and Ω are the pipe length and the circular frequency of the pipe respectively.

The dimensionless lateral displacement $\eta(\xi, \tau)$ can be written as follows:

$$\eta(\xi, \tau) = a_m(\tau)\Phi_m(\xi), \tag{5}$$

where Φ_m is the dimensionless mth mode of the pipe under the specified boundary condition and a_m ($= e^{j\omega\tau}\Psi$, where $j = \sqrt{-1}$ and Ψ is a constant) is a function of dimensionless time only.

By inserting equation (5) into equation (4), the dimensionless governing equation becomes

$$\left[\left\{1 + \sum_{i=1}^{M}\alpha_i\delta(\xi - \xi_i)\right\}\Phi_m(\xi) - \sum_{i=1}^{M}\mu_i\delta'(\xi - \xi_i)\Phi'_m(\xi) - \sum_{i=1}^{M}\mu_i\delta(\xi - \xi_i)\Phi''_m(\xi)\right]$$

$$\ddot{a}_m(\tau) + 2\mu\beta^{1/2}\Phi'_m(\xi)\dot{a}_m(\tau) + \{\Phi''''_m(\xi) + u^2\Phi''_m(\xi)\}a_m(\tau) = 0. \tag{6}$$

Applying Galerkin's method [5] for the analysis, equation (5) can be expressed as follows:

$$\eta(\xi, \tau) = \sum_{m=1}^{\infty} a_m(\tau)\phi_m(\xi), \tag{7}$$

where $\phi_m(\xi)$ is the dimensionless mode shape function of a pipe without fluid and concentrated masses [11].

Introducing the orthogonality of the functions, multiplying equation (10) by $\Phi_n(\xi)$, and integrating it about ξ from $\xi = 0$ to 1, we finally obtain the governing equation in the matrix form,

$$[A_{mn}]\ddot{a}_m(\tau) + [B_{mn}]\dot{a}_m(\tau) + [C_{mn}]a_m(\tau) = 0. \tag{8}$$

Through some matrix calculations equation (8) can be changed to the following simple form:

$$[f(v)]\{\Psi\} = \{0\}, \tag{9}$$

where $v = -\mathrm{j}\omega$.

Equation (9) has a non-trivial solution only if the characteristic determinant, i.e., the determinant of the matrix $[f(v)]$ vanishes. Generally, dimensionless eigenvalues of the determinant have its real and imaginary parts as follows:

$$\omega = \omega_R + \omega_I. \tag{10}$$

The dimensionless real component, ω_R, corresponds to the frequency of oscillation whereas the dimensionless imaginary component, ω_I, is associated with stability of the system. It is seen that the system is subject to a large number of stabilities, in the regions over which $\omega_I < 0$, by bucking if $\omega_R = 0$, and by flutter if $\omega_R \neq 0$ [10].

3. RESULTS AND DISCUSSION

Figure 2 shows variation of the first three natural frequencies for the fluid-conveying pipes as a function of the fluid velocity. As shown in the figure, introduction of rotary inertia causes much change for the second and third natural frequencies while it has relatively small influence on the first natural frequency. For example, the ratios between two natural frequencies with and without rotary inertia (i.e., $\omega_{with}/\omega_{without}$) for the clamped–clamped pipe with the fluid velocity $u = 2{\cdot}0$ are 0·430 and 0·886 for the third and first natural frequencies, respectively. For the same parametric values the effect of rotary inertia for the clamped–clamped pipe can be identified as the most visible among the three pipe boundary conditions. With increasing flow, the natural frequencies of all the modes vanish in turn, indicating the onset of buckling in the corresponding modes of the system. The values of the real frequencies (ω_R) have 0 as the fluid velocities, (u) have π, 2π, and 3π for the supported–supported, 4·49, 7·73, and 10·91 for the clamped–supported, and 2π, 8·99, 12·57 for the clamped–clamped pipe. Once a natural frequency attains a zero value, instability of the system begins and the fluid velocity in that case can be defined as a threshold (critical) velocity. Since $\omega_R = 0$ and $\omega_I < 0$ as the fluid velocities increase more than the critical

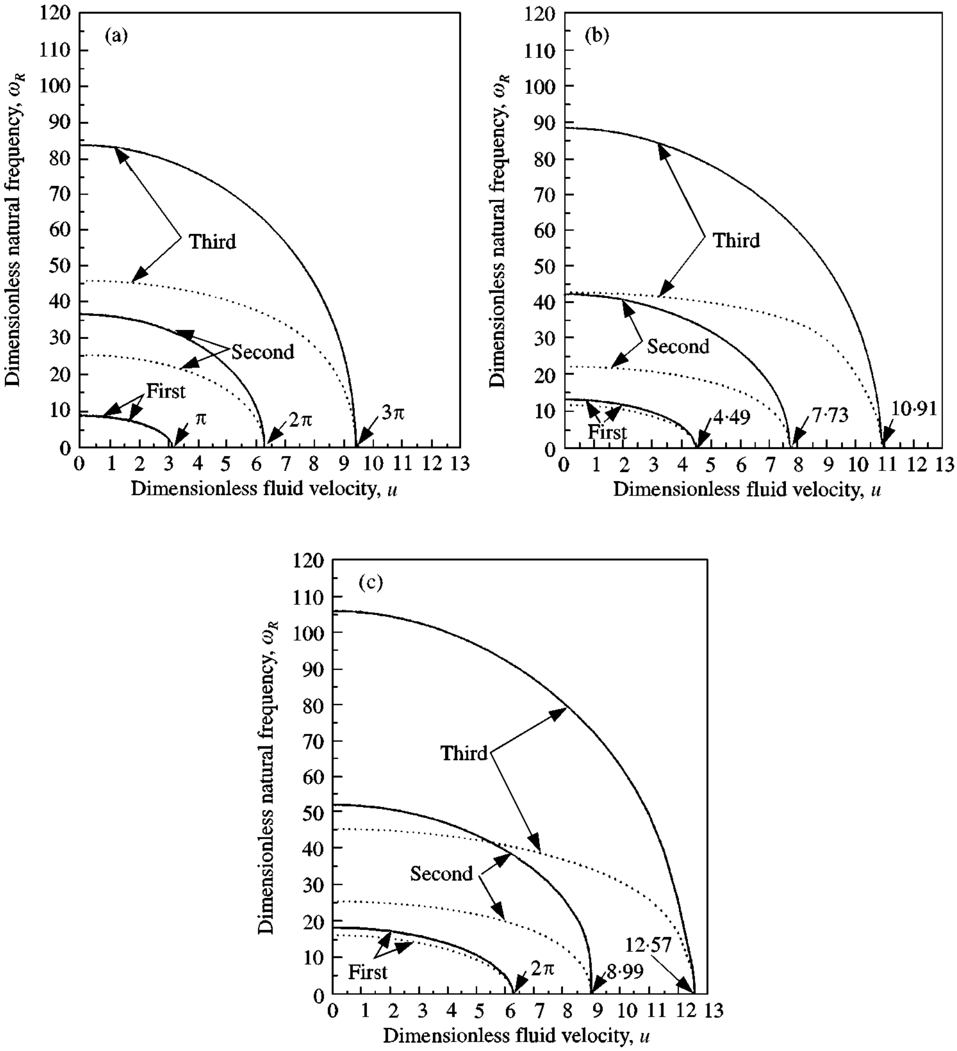

Figure 2. Natural frequency variation due to fluid velocity change. $\alpha_1 = 0{\cdot}2$, $\alpha_2 = 0{\cdot}1$, $\beta = 0{\cdot}2$, $\mu_1 = 0{\cdot}018$, $\mu_2 = 0{\cdot}025$, $\xi_1 = 0{\cdot}3$, $\xi_2 = 0{\cdot}5$. (a) Supported–supported; (b) clamped–supported; (c) clamped–clamped: ——, without rotary inertia ......, with rotary inertia.

velocities, the pipes assumed for the analysis bow out and buckle when the flow velocity exceeds the critical velocity. Through the analysis it is identified that the consideration of rotary inertia cannot change the critical fluid velocities suggested by Paidoussis and Issid [12] and Laura *et al.* [13] for the fluid-conveying pipe without concentrated masses.

Figure 3 shows the relation between the value of rotary inertia, μ_1, and the first three natural frequencies. For the analysis, a concentrated mass ($\alpha_1 = 1{\cdot}0$) is assumed to be at $0{\cdot}3L$ (i.e., $\xi_1 = 0{\cdot}3$ of the pipe and its rotary inertia is changed from $\mu_1 = 0{\cdot}0$ to 0·5. As shown in the figure, the consideration of rotary inertia produces much change on the natural frequencies. Its effect on the change of the natural frequencies is visible as μ_1 has a small value (i.e., less than 0·1 for the present case). Further increase of μ_1 causes the second and third natural frequencies to converge stationary values (e.g., nearly 35·0 and 19·0, respectively, for the second and third natural frequencies of the clamped–supported pipe).

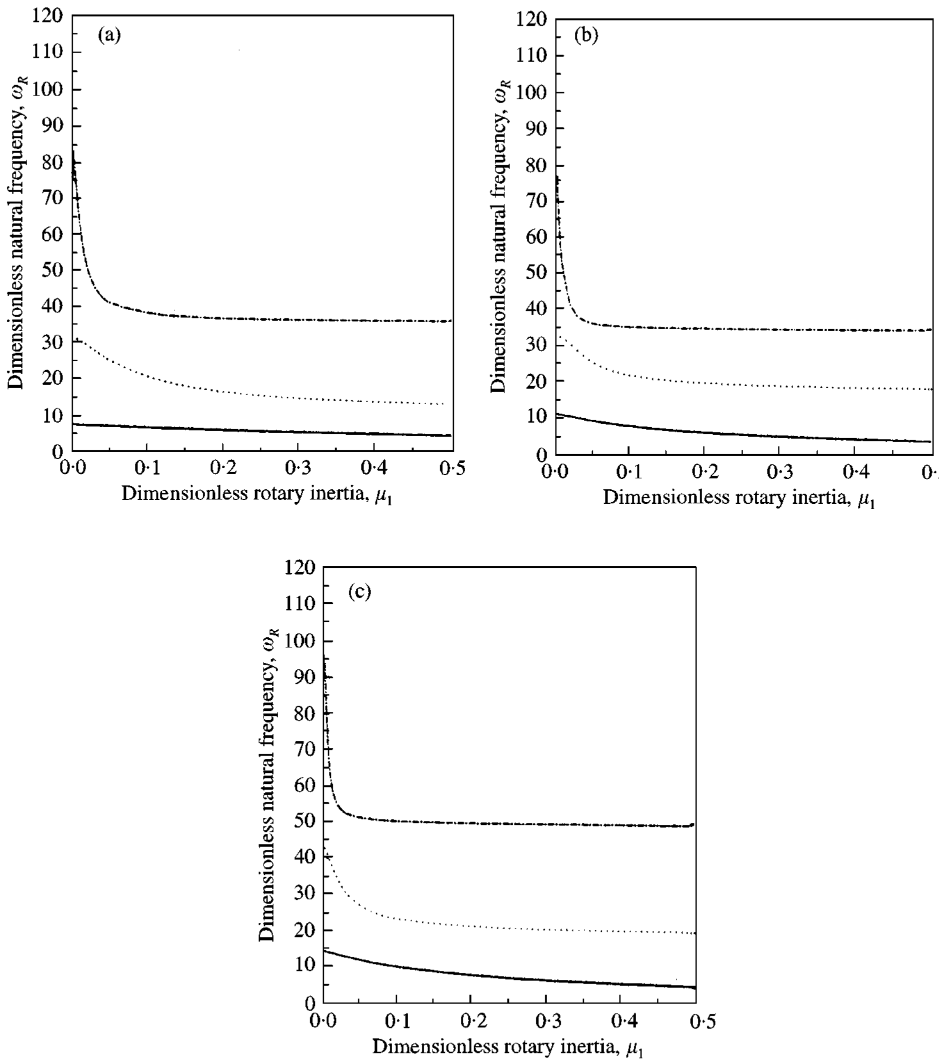

Figure 3. Rotary inertia versus natural frequency; $u = 0{\cdot}5$, $\alpha_1 = 1{\cdot}0$, $\beta = 0{\cdot}2$, $\xi_1 = 0{\cdot}3$. (a) Supported–supported; (b) clamped–supported; (c) clamped–clamped: ——, First; ......, Second; - · - · - · - ·, Third.

However, the value of the first natural frequency is almost linearly decreasing as the value of rotary inertia μ_1 starts increasing.

The combined effects of rotary inertia, μ_1, and the location of a concentrated mass, ξ_1, on the natural vibrations of the three boundary conditions have been determined and some results are shown in Figure 4. For the clamped–supported pipe, the values of the natural frequencies between two cases of $\xi_1 = 0{\cdot}0$ and $1{\cdot}0$ are much different from each other due to the different pipe end conditions. The location of the largest difference between two natural frequencies with and without rotary inertia is dependent on the pipe boundary conditions. For the second natural frequency, the locations are 0·5 for the clamped–clamped pipe, 0, 0·5, and 1·0 for the supported–supported pipe, and 0·56 and 1·0 for the clamped–supported pipe. Moreover, with considering rotary inertia, the second natural frequency approaches the first natural frequency without rotary inertia as ξ_1 approaches mid-span of the pipe.

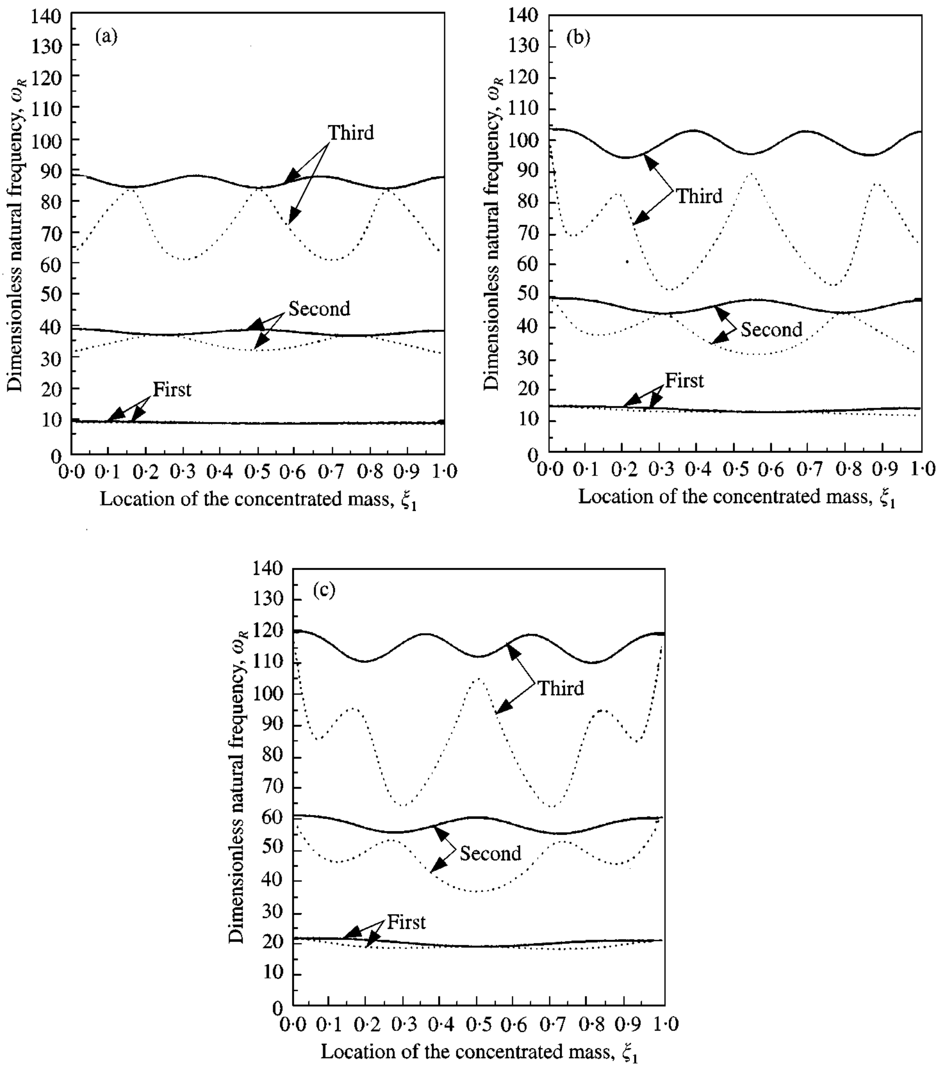

Figure 4. Natural frequency variation due to change of the location of the concentrated mass. $u = 1{\cdot}0$, $\alpha_1 = 0{\cdot}1$, $\beta = 0{\cdot}5$, $\mu_1 = 0{\cdot}01$. (a) Supported–supported; (b) clamped–supported; (c) clamped–clamped: ——, without rotary inertia: ......, with rotary inertia.

Figure 5 depicts the natural mode shapes of the system for the case of having two concentrated masses ($\alpha_1 = 1{\cdot}0$ and $\alpha_2 = 0{\cdot}2$). The heavier one is located at $\xi = 0{\cdot}1$ and the lighter one is at $\xi = 0{\cdot}5$. As shown in the figures, rotary inertia produces relatively small change on the first mode shape while it causes much change on the second and third mode shapes. The trend is the same regardless of pipe boundary conditions. By introducing rotary inertia, the number of nodes and its location can be changed. There is no fixed node at the second mode shape of the clamped–supported and clamped–clamped pipes when the rotary inertia effect is included into the analysis. Moreover, the number of the nodes for the third natural mode shapes for the three boundary conditions are reduced to 1 with including rotary inertia effect into the analysis.

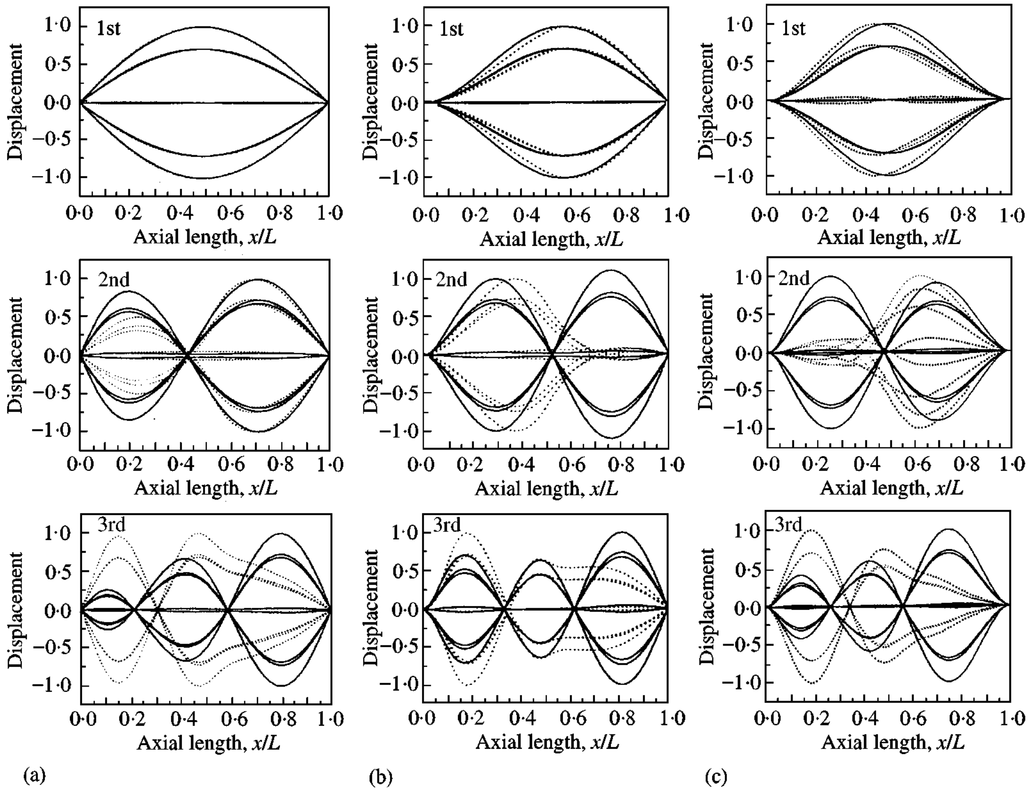

Figure 5. Natural mode shapes; $u = 0{\cdot}5$, $\alpha_1 = 1{\cdot}0$, $\alpha_2 = 0{\cdot}2$, $\beta = 0{\cdot}4$, $\mu_1 = 0{\cdot}01$, $\mu_2 = 0{\cdot}05$, $\xi_1 = 0{\cdot}1$, $\xi_2 = 0{\cdot}5$. (a) Supported–supported; (b) clamped–supported; (c) clamped–clamped: ——, without rotary inertia; ......, with rotary inertia.

REFERENCES

1. Y. U. CHEN 1961 *ASME, Journal of Applied Mechanics* **30**, 310–311. On the vibration of beams or rods carrying a concentrated mass.
2. W. H. HOPPMANN 1952 *ASME, Journal of Applied Mechanics* **19**, 301–307. Forced lateral vibration of beam carrying a concentrated mass.
3. J. C. MALTBAEK 1961 *International Journal of Mechanical Sciences* **3**, 197–218. The influence of a concentrated mass on the free vibrations of a uniform beam.
4. K. SATO, H. SAITO and K. OTOMI 1978 *ASME, Journal of Applied Mechanics* **45**, 634–648. The parametric response of a horizontal beam carrying a concentrated mass under gravity.
5. J. L. HILL and C. P. SWANSON 1970 *ASME, Journal of Applied Mechanics* **37**, 494–497. Effects of lumped masses on the stability of fluid conveying tubes.
6. S. S. CHEN and J. A. JENDRZEJCZYK 1985 *Journal of Acoustical Society of America* **77**, 887–895. General characteristics, transition, and control of instability of tubes conveying fluids.
7. T. T. WU and P. P. RAJU 1974 *ASME, Journal of Pressure Vessel Technology* **96**, 154–158. Vibration of a fluid conveying pipe carrying a discrete mass.
8. H. H. PAN 1965 *ASME, Journal of Applied Mechanics* **32**, 434–437. Transverse vibration of an Euler beam carrying a system of heavy bodies.
9. M. N. HAMDAN and M. H. F. DADO 1997 *Journal of Sound and Vibration* **206**, 151–168. Large amplitude free vibrations of a uniform cantilever beam carrying an intermediated lumped mass and rotary inertia.
10. R. D. BLEVINS 1977 *Flow-Induced Vibration*. New York: Van Nostrand Reinhold Company.

11. R. D. BLEVINS 1979 *Formulas for Natural Frequency and Mode Shape*. New York: Van Nostrand Reinhold Company.
12. M. P. PAIDOUSSIS and N. T. ISSID 1974 *Journal of Sound and Vibration* **33**, 267–294. Dynamic stability of pipes conveying fluid.
13. P. A. A. LAURA, G. M. FICCADENTI DE IGLESIAS and P. L. VERNIERE DE IRASSAR 1987 *Applied Acoustics* **21**, 191–198. A note on flexural vibrations of a pipeline containing flowing fluid.